PHYSICAL REVIEW D **113,** 063560 (2026)

Cosmology with a nonlinear barotropic Israel-Stewart fluid with causal relaxation time

Vishnu A Pai[*] and Titus K Mathew[†]

Department of Physics, Cochin University of Science and Technology, Cochin-682022, Kerala, India

(Received 7 January 2026; accepted 4 March 2026; published 24 March 2026)

We derive an extended expression for the relaxation time of a barotropic Israel-Stewart (IS) fluid (BISF) using the nonlinear causality constraint, and propose a new formulation for modeling causal bulk viscous dissipation in barotropic fluids in the full nonlinear regime. With this generalized relaxation time, the covariant nonlinear IS equation reduces to a first-order nonlinear differential equation relating the bulk viscous pressure and the energy density, which remains valid in any homogeneous and isotropic spacetime. In a spatially flat Friedmann universe, adopting this extended relation within the generalized nonlinear IS theory yields a new class of analytical solutions in both the linear and certain truncated nonlinear regimes. We also find that the resulting effective equation of state in the linear regime naturally reproduces the generalized polytropic form often introduced phenomenologically in the literature. The dynamical implications of adopting the causal relaxation time for BISF are investigated in the linear, truncated nonlinear, and full nonlinear far-from-equilibrium regimes, and the constraints required to ensure physically viable evolution of the viscous fluid are derived. A detailed dynamical systems analysis of the coupled Einstein-Israel–Stewart (EIS) system is also performed. Finally, we solve the coupled EIS equations numerically in the full nonlinear regime and show that the model can support a transient Hubble slow-roll expansion phase with a smooth exit to a radiation-dominated universe, which is challenging to obtain in standard inflationary models.

DOI: 10.1103/pyht-c2jt

I. INTRODUCTION

Relativistic dissipative hydrodynamics provides the theoretical foundation for describing and modeling nonequilibrium processes in relativistic fluids, encompassing applications from the early Universe to relativistic heavy-ion collisions and compact astrophysical objects [1–3]. In cosmology, it has been shown that, bulk viscous stresses can contribute to entropy generation [4], particle creation [5], and the damping of anisotropies in the early Universe [6,7]. Moreover, it was also shown that, under suitable conditions, an interacting multicomponent medium can be recast as an effective bulk viscous fluid [8,9]. These profound cosmological implications of bulk viscosity have attracted considerable attention, particularly its ability to drive acceleration expansion of the Universe [10–13].

The theoretical formulation of relativistic dissipative fluid dynamics has undergone substantial development over the past decades. The earliest approaches, due to Eckart [14] and later Landau and Lifshitz [15], were based on first-order constitutive relations connecting the thermodynamic fluxes to gradients of macroscopic variables. However, in spite of being a direct relativistic extension of the standard Navier-Stokes relation, these formulations were shown to violate causality [16] and predict solutions with unstable final equilibrium states [17]. To overcome these drawbacks, Israel and Stewart generalized the above approach by considering second-order corrections with additional relaxation type degree of freedoms in the entropy flux equation [16,18]. The resulting formulation, called the Israel-Stewart theory (IS), forms a thermodynamically consistent framework with relaxation-type equations for viscous pressure, which ensures causality within the near-equilibrium limit. However, the IS theory did not provide a general proof of causality and stability for fluids, that are driven far from equilibrium, or when nonlinear dissipative effects are dominant. This long-standing problem was recently solved in [19], where the authors derived the necessary and sufficient conditions under which causality, stability, and hyperbolicity are satisfied in general nonlinear IS theories that are dynamically coupled to Einstein equations. This established the mathematical consistency of relativistic hydrodynamics beyond the linear regime, and provided a robust foundation for studying strongly nonequilibrium phenomena in relativistic hydrodynamic systems. Accordingly, an interesting phenomenological dissipative fluid model was recently proposed, which is argued to be viable even the system undergoes rapid expansions and contractions [20].

[*]Contact author: vishnuajithj@gmail.com, vishnuajithj@cusat.ac.in

[†]Contact author: titus@cusat.ac.in

Even though the causality conditions can ensure the mathematical consistency of nonlinear IS theories, a valid realization of the framework requires specifying the functional form of the non-linear dissipative contribution. This choice is particularly important when relativistic fluids undergo large departures from local equilibrium, since nonlinear dissipative effects can play a significant role in governing the dynamics of the fluid in the far from equilibrium regime. In the relativistic settings, where rapid expansion/contraction can both influence and be influenced by the evolution of dissipative stresses, a consistent treatment of nonlinearities is therefore essential. This motivates the adoption of generalized, nonpolynomial formulations of the IS equations that remain well defined for arbitrarily large deviations from equilibrium while reducing smoothly to the standard IS structure in the near-equilibrium limit. In this article, we implement such a formulation by introducing an explicit exponential nonlinear dissipative contribution.

Despite its wide ranging applications, in most cases, IS framework in its standard formulation requires phenomenological prescriptions for the relaxation time (τ) and the viscous coefficient (ζ), particularly in cosmological settings. In most cases, the dissipative variables are considered to be barotropic, and are hence modeled as a function of the fluid's energy density [21–23]. While these basic assumptions greatly simplify analytical and numerical calculations, it generally does not ensure that the resulting theory respects causality. The first explicit causal relation for the relaxation time was derived by Maartens in [24], which established a direct connection between dissipative variables within the near-equilibrium regime. However, since this relation is obtained under the assumption of small deviations from equilibrium, adopting the same relation in far-from-equilibrium regimes may not ensure causality. In cosmological contexts, where rapid expansion and significant departures from local equilibrium may occur, these simplifications can affect the accurate modeling of bulk dissipative processes [25–27]. Furthermore, it is to be noted that viscous driven accelerated expansion of the Universe is an inherently far-from-equilibrium behavior. Hence, relaxation dynamics of relativistic dissipative fluids in cosmology necessarily requires a reexamination subject to the general causality framework derived in [19].

In this work, we derive an extended expression for the relaxation time of a barotropic, nonlinear IS fluid directly from the general causality condition proposed in [19], such that the resulting formulation guarantees causality under arbitrary departures from equilibrium. We will show that, for a barotropic fluid, adopting the aforementioned expression for relaxation time reduces the IS equation into a first-order nonlinear ordinary differential equation connecting the bulk viscous pressure and the energy density, which is valid in any homogeneous and isotropic spacetimes. This reduction renders the theory analytically tractable while also preserving the necessary causal structure. We will then apply this IS equation in the context of spatially flat FLRW spacetime, and show that this formulation yields new class of exact analytical solutions that resembles the generalized polytropic equations of states, which are often introduced phenomenologically [28–32]. Finally, we will also show that, the resulting dynamical equation can also enable a transient viscous driven early-inflationary phase that naturally transitions into radiation-dominated epoch and remains observationally consistent.

II. NON-LINEAR ISRAEL-STEWART THEORY WITH CAUSAL RELAXATION TIME

In homogeneous and isotropic spacetimes, one defines the energy momentum tensor and particle flux density of dissipative fluids with energy density "ρ," nonequilibrium pressure "$\mathcal{P}$," particle number density "$\mathfrak{n}$," as,

$$T^{\mu\nu} = \rho u^\mu u^\nu + (p + \Pi)\Delta^{\mu\nu} \quad : \quad \mathfrak{n}^\mu = \mathfrak{n} u^\mu. \tag{1}$$

Here, p is the equilibrium pressure, Π represents the bulk viscous pressure, u^μ is the particle four-velocity in the instantaneous comoving frame, $\Delta_{\mu\nu} = g_{\mu\nu} + u_\mu u_\nu$ is the projection tensor orthogonal to u_μ, and $g^{\mu\nu}$ is the space-time metric. In general relativity, the equations of motion that govern the dynamics of such a fluids are [19],

$$u^\mu \nabla_\mu \rho = -(\rho + p + \Pi)\nabla_\mu u^\mu, \tag{2}$$

$$u^\mu \nabla_\mu u_\nu = -\frac{[\omega_\rho \Delta^\mu_\nu \nabla_\mu \rho + \omega_\mathfrak{n} \Delta^\mu_\nu \nabla_\mu \mathfrak{n} + \Delta^\mu_\nu \nabla_\mu \Pi]}{\rho + p + \Pi}, \tag{3}$$

$$u^\mu \nabla_\mu \mathfrak{n} = -\mathfrak{n} \nabla_\mu u^\mu, \tag{4}$$

$$u^\mu \nabla_\mu \Pi = -\frac{1}{\tau_\Pi}[\Pi e^{\lambda \Pi} + \zeta_\Pi \nabla_\mu u^\mu]. \tag{5}$$

Here, $(\omega_\rho, \omega_\mathfrak{n}, \zeta_\Pi, \tau_\Pi, \lambda)$ are free parameters of the model that depend on the nature of the fluid. To be precise, $\omega_\rho = (\partial p/\partial \rho)_\mathfrak{n}$ is the squared adiabatic speed of sound in the medium, $\omega_\mathfrak{n} = (\partial p/\partial \mathfrak{n})_\rho$ quantifies the dependence of pressure on particle number density, "τ_Π" represents the relaxation time of the fluid, "ζ_Π" is the coefficient of bulk viscosity, and "λ" is the constant nonlinear coupling parameter (Note that "λ" has the dimension of inverse energy density). In general, the parameters τ_Π and ζ_Π can have explicit dependence also on $(\rho, \mathfrak{n}, \Pi)$.

Transport equation (5) represents a fully nonlinear generalization of the standard Israel-Stewart relation, characterized by the explicit inclusion of an exponential function of Π in addition to the standard IS structure. This formulation effectively captures all the higher-order dissipative contributions within a closed functional form, thereby enabling the theory to be consistently extended to arbitrarily far-from-equilibrium regimes. In the near-equilibrium limit, the above equation reduces to,

$$u^\mu \nabla_\mu \Pi = -\frac{1}{\tau_\Pi}[\Pi + \lambda\Pi^2 + \mathcal{O}(\Pi^3)\ldots + \zeta_\Pi \nabla_\mu u^\mu]. \quad (6)$$

If you truncate this relation by considering up to second order in Π, then the resulting relation exactly matches the nonlinear form of IS equation proposed in [19]. Hence, Eq. (5) becomes an extended form of the nonlinear Israel-Stewart relation proposed therein. Notably, the above equation exactly reduces to Maxwell-Cattaneo relation when $\lambda = 0$, and when $\lambda \neq 0$, it becomes a fully nonlinear extension of the same. In addition to this, if the limit $\tau_\Pi \to 0$ is also satisfied, the proposed relation approaches the relativistic Navier-Stokes relation. This extended form of IS equation (5) not only captures the necessary physical characteristics of the system, but can also provide exact analytical solutions in Friedmann-Lemaître-Robertson-Walker (FLRW) spacetime in the linear cases, and also in certain truncated nonlinear cases, which is discussed in the next section. Finally, one can show that in the Minkowski spacetime, this extended, fully nonlinear Israel-Stewart relation offers a stable equilibrium solution, refer to Appendix A.

To complete the system, one must then express the dissipative variables $(\omega_\rho, \omega_\mathfrak{n}, \zeta_\Pi, \tau_\Pi)$ in terms of the independent variables. Ideally, these relations should be derived from underlying microscopic interactions in the fluid. However, in most cases such a description is not readily obtained, and consequently one can postulate these relations phenomenologically.

In the general case of a barotropic bulk viscous fluid both, the equilibrium pressure, and the viscous pressure, depend only on the energy density of the fluid (and not on the particle number density), and hence one often adopts the relations; $\Pi = \Pi(\rho)$, and $p = w_0\rho$. Here, w_0 is considered to be a constant free parameter (related to adiabatic speed of sound in the medium, i.e., $w_0 = c_s^2$), though in general, it can also vary with energy density. It is then easy to see that, owing to this choice of pressure we get, $\omega_\rho = w_0$ and $\omega_\mathfrak{n} = 0$. However, obtaining the form of ζ_Π and τ_Π is not that straightforward. In the linear regime, authors most often consider two different approaches in choosing ζ and τ; One either treats them as independent barotropic variables [33,34], or alternatively, one relates them via the causality constraint in the linear regime [24], and subsequently, postulates a barotropic bulk viscous coefficient [35]. Regardless, in the nonlinear regime, or in the cases where when τ and ζ_Π are allowed to depend also on Π, both these cases may fail to satisfy causality. This is because, the linear constraint may not be applicable in the nonlinear regime. Hence, in such cases one must replace the linear causality constraint with the nonlinear version derived in [19]. In that manuscript, authors proved that the set of equations (2)–(5), coupled to the Einstein's field equation, represents a first-order symmetric hyperbolic system that is causal, stable, and hyperbolic in the nonlinear regime, provided the constraint given below is satisfied;

$$\left[\frac{\zeta_\Pi}{\tau_\Pi} + \mathfrak{n}\omega_\mathfrak{n}\right]\frac{1}{\rho + p + \Pi} + \omega_\rho \leq 1. \quad (7)$$

The left-hand side of the above inequality represents the effective squared speed of sound in the dissipative fluid, and hence the constraint basically suggests that $c^2_{\text{acoustic}} \leq c^2$, where "$c$" is the cosmic speed limit. For the barotropic case considered here, with $p = w_0\rho$, we have $\omega_\mathfrak{n} = 0$ and $\omega_\rho = w_0$. The causality constraint then reduces to a bound on the viscous contribution to the total acoustic speed, analogous to the analysis performed in the linear regime [24,36]. To implement this constraint in a simple and transparent manner, we parametrize the bound by introducing a dimensionless constant $0 < \epsilon_0 \leq 1$, which quantifies how close the system operates to the causal limit. This directly determines the relaxation time as,

$$\tau_\Pi = \frac{\zeta_\Pi}{\epsilon_0(1 - w_0)(\rho + p + \Pi)} \quad ; \quad 0 < \epsilon_0 \leq 1. \quad (8)$$

For a detailed derivation, see Appendix B. Since the above definition of the relaxation time is directly derived from the causality constraint, the transport equation for bulk viscosity will remain causal at all times, even when fluid is far from equilibrium, i.e., $|\Pi| \approx (\rho + p)$. Consequently, we will refer to this version of relaxation time as the "causal relaxation time" (τ_c) and the associate fluid as BISF, i.e., barotropic Israel Stewart fluid. Interestingly, this equation exactly reduces to standard relation in the linear regime when the fluid is in a near-equilibrium state, i.e., when $|\Pi|/(\rho + p) \ll 1$, and can hence be considered as an extended version of the linear relation. The fully nonlinear IS equation proposed in Eq. (5), can show both pseudo-plastic as well as viscoelastic behavior in the appropriate regimes, for details refer to Appendix C.

In the far from equilibrium regime, $|\Pi| \to \rho + p$, and as a result τ_c increases significantly and may even diverge if $|\Pi| = \rho + p$. To bypass this singularity, one must propose a suitable initial condition for the fluid, and constrain the free parameters in the model, such that the obtained solution predicts an acceptable causal evolution for the viscous fluid (i.e., $|\Pi| < \rho + p$ at all times). Therefore, adopting the causal relaxation time given in Eq. (8) directly leads to the following results:

(i) Viscous driven de-Sitter expansion is a theoretical impossibility since $\rho + p + \Pi = 0$ is nonachievable. However, a quintessence solution mimicking a quasi–de Sitter phase is plausible when, $\Pi \approx -(\rho + p)$.

(ii) Phantom viscous fluids are also theoretically non-feasible. This is because, in the present case, the fluid must satisfy the constraints, $\rho + p + \Pi \geq 0$,

$w_0 \geq 0$, and $\zeta_\Pi \geq 0$, at all times to ensure causality and uniqueness of solution [19].

Combining the equations (2), (5), and (8), we obtain the following nonlinear ordinary differential equation (ODE) for a barotropic fluid,

$$\frac{d\Pi}{d\rho} = \epsilon_0(1 - w_0)\left[1 + \frac{\Pi e^{\lambda\Pi}}{\zeta_\Pi \nabla_\mu u^\mu}\right]. \tag{9}$$

This ODE is quite general as it is independent of the choice of space-time metric, and was obtained as a direct consequence of the two assumptions; (a) the bulk viscous pressure is barotropic (b) the relaxation time is given by Eq. (8). In the upcoming section, we will analyze the behavior of this equation in the cosmological setting by considering both linear and nonlinear effects.

III. FLRW UNIVERSE WITH BISF

Consider a spatially flat, homogeneous and isotropic universe, in which the ideal fluid is replaced by the BISF modeled in the above section. Substituting the standard Friedmann-Lemaître-Robertson-Walker metric given as,

$$ds^2 = -dt^2 + a(t)^2[dx^2 + dy^2 + dz^2], \tag{10}$$

in the Einstein's field equations, and using Eqs. (1), (10), we get the modified Friedmann equations,

$$3H^2 = \rho, \tag{11}$$

$$2\dot{H} + 3H^2 = -(p + \Pi). \tag{12}$$

Since we are considering a barotropic viscous pressure, the dissipative coefficient ζ_Π must also be barotropic, i.e., $\zeta_\Pi \sim \zeta_\Pi(\rho)$. The simplest, most straightforward ansatz that one could consider is then, $\zeta_\Pi(\rho) = \zeta_0\sqrt{\rho^{2n+1}}$, which is a popular form often considered in literature [24].[1] Adopting this relation in Eq. (9), we obtain,

$$\frac{d\Pi}{d\rho} = \epsilon + \eta\left[\frac{\Pi e^{\lambda\Pi}}{\rho^{n+1}}\right]. \tag{13}$$

Here, we have denoted $\epsilon = \epsilon_0(1 - w_0)$, $\eta = \epsilon/\sqrt{3}\zeta_0$, and ϵ_0 and ζ_0, are constant positive real numbers. Also it is evident from Eq. (8) that for satisfying the causality; $0 < \epsilon \leq 1$ if $w_0 = 0$, and $0 < \epsilon \leq 2/3$ if $w_0 = 1/3$.

To solve this nonlinear ODE, one needs to impose a suitable initial condition, and in cosmological context, the natural intuition is that the fluid starts off from an out-of-equilibrium state, and later approaches a stable equilibrium as it evolves in time. Therefore, it is expected that the end phase solution is a stable equilibrium state where the bulk dissipative fluxes necessarily vanish. In this article we will adhere to this intuitive picture. Hence, we consider the fluid to evolve from an initial far-from-equilibrium state with $\rho = \Lambda_e$ and $\Pi_e = -\mathfrak{w}\Lambda_e$ toward a late-time stable state in which both ρ and Π vanish. Physical consistency demands that acceptable solutions satisfy, $\Pi/\rho \to -\kappa$, with $\kappa \gtrapprox 0$, as $a \to \infty$ and $\rho \to 0$. Here, the parameter "$\mathfrak{w}$" measures the initial deviation from equilibrium, and its value is bounded within the limits $0 \leq \mathfrak{w} < 1 + w_0$, as dictated by the null energy condition, $\rho + p + \Pi \geq 0$.

We will now investigate the evolution of the BISF in both the linear and nonlinear regime and determine the physically acceptable solutions, which predict a fluid that is relaxing to its equilibrium state. In the linear regime we will consider both $n = 0$ and $n \neq 0$ cases, while in the nonlinear regime we will confine our analysis to the $n = 0$ case only, this reduces the number of free parameters and significantly simplifies the nonlinear equation.

A. BISF in the linear regime

In the linear regime ($\lambda = 0$, or when $|\lambda\Pi| \to 0$), the nonlinear IS equation reduces to the Maxwell-Cattaneo relation,

$$\frac{d\Pi}{d\rho} = \epsilon + \eta\left[\frac{\Pi}{\rho^{n+1}}\right]. \tag{14}$$

This simple equation can be exactly solved to obtain the analytical solutions for cases (a) $n = 0$, and (b) $n \neq 0$,

(a) For $n = 0$: In this case we get,

$$\Pi = \left[\frac{\epsilon}{1 - \eta}\right]\rho + \mathbb{C}\rho^\eta. \tag{15}$$

Interestingly, the above equation connecting the viscous pressure with energy density is identical to the equation of state of a generalized polytroic fluid [28–32]. Applying the initial condition $\Pi_e = -\mathfrak{w}\Lambda_e$ at $\rho = \Lambda_e$, we get the exact solution as,

$$\frac{\Pi}{\rho} = \frac{\epsilon}{1 - \eta} - \left[\mathfrak{w} + \frac{\epsilon}{1 - \eta}\right]\left[\frac{\rho}{\Lambda_e}\right]^{\eta - 1} \quad ; \quad \eta \neq 1. \tag{16}$$

By analyzing this equation, significant inferences can be drawn regarding the possible behaviors that the fluid could show, and one can assess which among them are physically viable ones. As mentioned earlier, the acceptable solutions are those in which the fluid is seen evolving toward the equilibrium state as the energy density dilutes. This means, as ρ evolves from Λ_e to zero, $|\Pi|/\rho$ must decrease from its initial value, and therefore, Π/ρ must tend to zero as $\rho \to 0$. To visualize this clearly, we make a 4D plot of the above

[1] Since n is an unspecified constant real number, one has the freedom to choose the power of ρ in the ansatz for viscous coefficient for better representation. Here we adopted $\sqrt{\rho^{2n+1}}$ so that final expression looks less tedious.

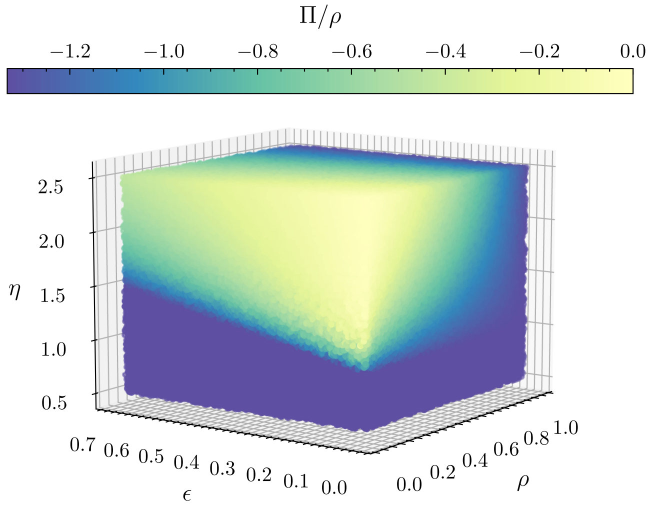

FIG. 1. 4D scatter plot depicting the evolution of Π/ρ for $n = 0$ case of BISF in the linear regime.

equation by considering ϵ, η and ρ as the three axes of a coordinate system, and plotting Π/ρ as a color gradient depicted via the color bar, as seen in Fig. 1. In the plot, we have fixed[2] $\Lambda_e = 1$ and $\mathfrak{w} = 1.33$. Based on the color map that we have used in the figures, the acceptability criterion stated above directly implies the following; as energy density (ρ) evolves from one to zero, the viable solutions are those for which the color gradates from dark blue to bright yellow. According to Fig. 1 we see that for having viable solutions, η must be sufficiently large, while ϵ should be necessarily small. As the value of ϵ increases, the value of η required for obtaining an acceptable solution becomes larger. At the same time, we also see that if the value of η becomes smaller than one, no value of ϵ (however small it may be), will yield a solution that is evolving toward equilibrium. Furthermore, if we consider $\eta < 1$, then from Eq. (15), we will obtain the scenario where, $\Pi/\rho \to -\infty$ as $\rho \to 0$, which is unacceptable. Hence in this case, for having a physically viable evolution for the bulk viscous fluid, it is mandatory that, $\eta > 1$ and $\epsilon \ll 1$. Also, in this domain of η and ϵ values, one can show that,

$$\lim_{\rho\to 0} \frac{\Pi}{\rho}\bigg|_{\eta>1} = \frac{\epsilon}{1-\eta}. \tag{17}$$

Therefore, "$\epsilon \ll 1$" is also essential to ensure that the viscous fluid is close to equilibrium state in the late phase.

(b) For $n \neq 0$: Surprisingly, Eq. (14) also offers an analytical solution for any arbitrary value of "n" except zero (in which case one uses the solution obtained in the previous case). This can be derived via the method of integrating factors, which yields,

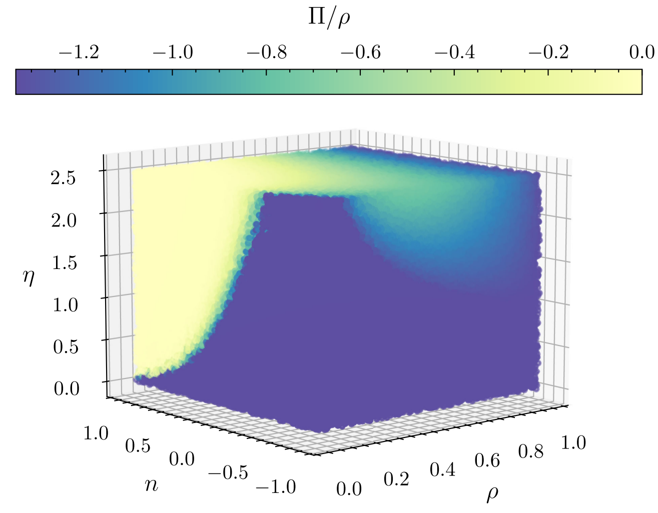

(a)

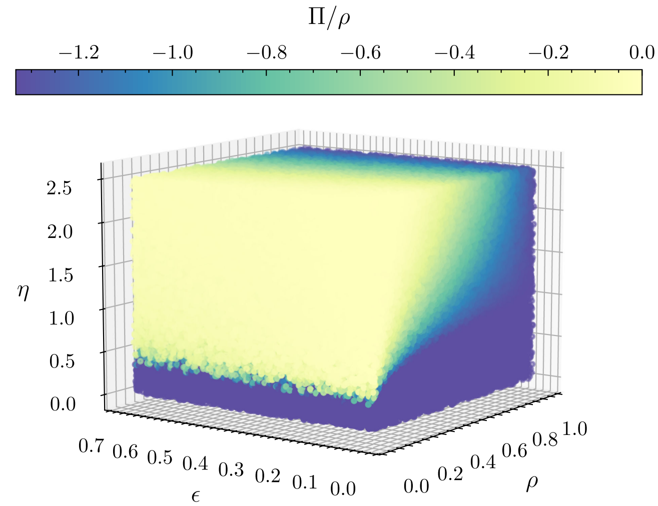

(b)

FIG. 2. 4D scatter plots showing the evolution of Π/ρ, for $n \neq 0$ linear case of BISF. (a) For different n and $\epsilon = 0.01$. (b) For different ϵ and $n = 0.50$.

$$\frac{\Pi}{\rho} = e^{-\eta/(n\rho^n)}\left\{\mathcal{E} - \left[\frac{\mathfrak{w}\Lambda_e}{\rho}\right] e^{\eta/(n\Lambda_e^n)}\right\}$$

$$\text{where, } \mathcal{E} = \frac{\epsilon}{\rho}\int_{\Lambda_e}^{\rho} e^{\eta/(n\tilde{\rho}^n)} d\tilde{\rho}. \tag{18}$$

Here we have used the same initial condition, as in the previous case, and have integrated within the limit (Λ_e, ρ). The exact behavior of this solution can be studied with the help of the plots in Fig. 2. To plot Fig. 2(a) we have taken the values, $\Lambda_e = 1$, $\mathfrak{w} = 1.33$, $\epsilon = 0.01$, and allowed "(n, η, ρ)" to vary. And for plotting Fig. 2(b) we fix $\Lambda_e = 1$, $\mathfrak{w} = 1.33$, $n = 0.50$ and vary "(ϵ, η, ρ)."

[2]We have considered the case where fluid is initialized near to its maximum possible out-of-equilibrium state $\mathfrak{w} \approx 1 + w_0$. Recall that maximum value of w_0 is $1/3$, which implies $\mathfrak{w} \approx 4/3$.

By analyzing the Figs. 2(a) and 2(b), we arrive at the following inferences;

(i) For $n < 0$, the viscous fluid initially evolves toward the equilibrium state [as indicated by a change in color from dark blue to bright yellow in Fig. 2(a)] but later, as ρ tends to zero, it is driven away from equilibrium state (as indicated by a color shift from bright yellow to dark-blue). This fact is true irrespective of the values of η and ϵ. Consequently, in this case, the dissipative fluid totally fails to approach equilibrium state in the late phase.

(ii) For $n > 0$, fluid can evolve toward equilibrium state, provided $\epsilon \ll 1$ and "η" is above a particular threshold, which in turn depends on the value of "n." From Figs. 2(a) and 2(b) it is clear that for $\epsilon \ll 1$; larger positive values of "n" can ensure viable solutions even for small η values. Hence, $\eta > 1$ is not a strict requirement to predict viable solutions in the cases where $n > 0$.

(iii) As $n \to 0$, the plot begins to align closely with the previous case in which $n = 0$, i.e., Fig. 1. As expected, from Fig. 2(a), we see that the inferences drawn in the earlier case will apply here also, i.e., viable solutions are obtained when, $\eta > 1$ and $\epsilon \ll 1$.

B. BISF in the truncated nonlinear regime

By truncating the nonlinear IS equation in Eq. (13) by considering only up to second order in Π, we obtain the reduced ODE (for $n = 0$),

$$\frac{d\Pi}{d\rho} = \epsilon + \eta\left[\frac{\Pi + \lambda\Pi^2}{\rho}\right]. \tag{19}$$

The reduced nonlinear ODE (19) can be exactly solved and the following analytical solution can be obtained;

$$\frac{\Pi}{\rho} = -\frac{2\epsilon}{\mathcal{A}}\left\{\frac{\Gamma[\eta]J_{\eta-1}[\mathcal{A}] + \mathbb{C}\Gamma[-\eta]J_{-(\eta-1)}[\mathcal{A}]}{\Gamma[\eta]J_{\eta}[\mathcal{A}] - \mathbb{C}\Gamma[-\eta]J_{-\eta}[\mathcal{A}]}\right\}, \tag{20}$$

$$\mathbb{C} = \frac{\Gamma[\eta]}{\Gamma[-\eta]}\left\{\frac{\mathcal{B}\mathfrak{w}J_{\eta}[\mathcal{B}] - 2\epsilon J_{\eta-1}[\mathcal{B}]}{\mathcal{B}\mathfrak{w}J_{-\eta}[\mathcal{B}] + 2\epsilon J_{-(\eta-1)}[\mathcal{B}]}\right\} \tag{21}$$

where we have denoted,

$$\mathcal{A} = 2\sqrt{\epsilon\eta\lambda\rho} \quad \text{and} \quad \mathcal{B} = 2\sqrt{\epsilon\eta\lambda\Lambda_e} \tag{22}$$

$$\Gamma[z] = \int_0^\infty k^{z-1}e^{-k}dk \quad \text{(gamma function)} \tag{23}$$

and, $J_x[y]$ represents the Bessel function of the first kind. Analysis of this equation leads to the following inferences;

(i) Presence of the gamma functions $\Gamma[\eta]$ and $\Gamma[-\eta]$ imposes a restriction on the parameter η, as the gamma function is undefined for negative integers. This is not that problematic since η represents a combination of ϵ_0, w, and ζ_0, rather than a single parameter, and it is highly improbable that η assumes integer values.

(ii) To ensure that $\mathcal{A}$, $\mathcal{B}$, and consequently Π/ρ, remain real valued, it is necessary that $\lambda > 0$.

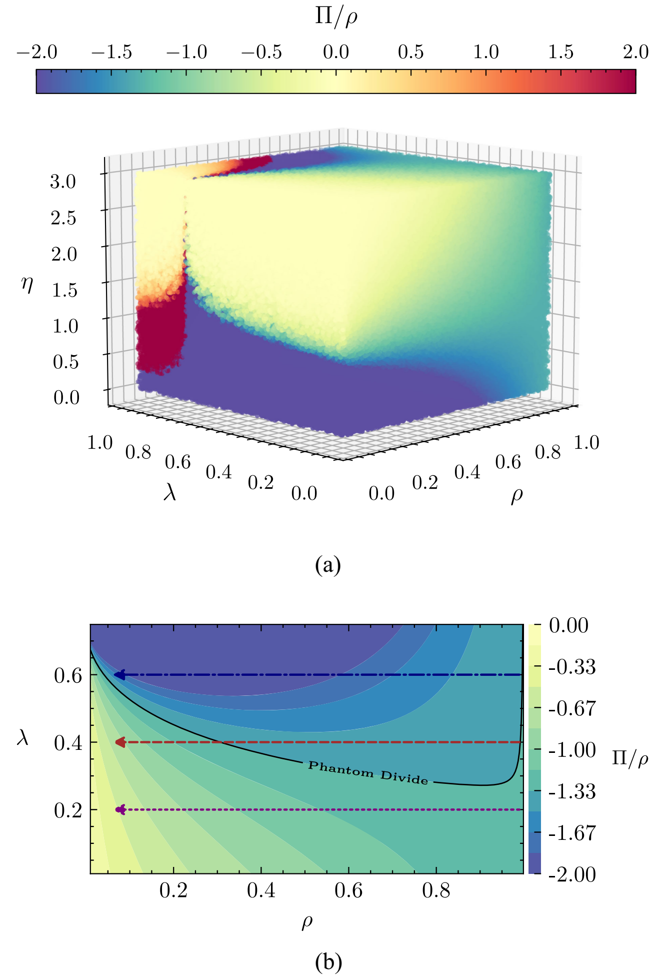

FIG. 3. These are contour and scatter plots showing the evolution of Π/ρ for truncated nonlinear case by considering $\Lambda_e = 1$, $\mathfrak{w} = 1.33$, and $\epsilon = 0.01$. (a) 4D scatter plot. (b) Contour plot obtained by slicing the above 4D scatter plot at $\eta = 1.50$. Here, phantom barrier is depicted as a solid black line.

As done in the previous cases, additional constraints on the model parameters are deduced by analyzing the conditions for viable solutions. This is done by referring to the plots 3(a) and 3(b). The arrows shown in the contour plot 3(b) represent the evolution trajectory of "Π/ρ" for given values of ϵ, $\mathfrak{w}$, η, and a particular λ: the blue arrow is for $\lambda = 0.6$, the red arrow is for $\lambda = 0.4$, and the purple arrow corresponds to $\lambda = 0.2$. For $\lambda \ll 1$, results obtained in the linear ($n = 0$) case become exactly applicable, i.e., acceptable solutions require, $\epsilon \ll 1$

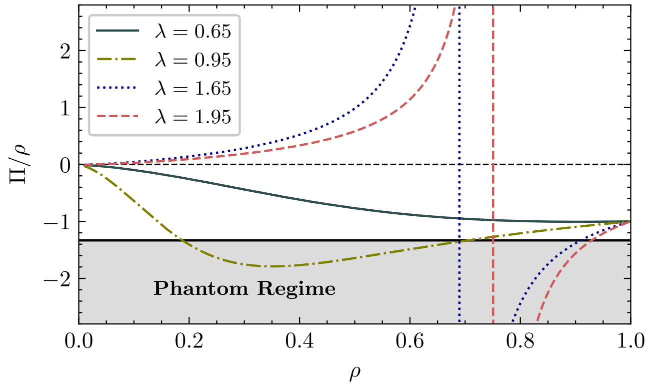

FIG. 4. Plot depicting the evolution of "Π/ρ" with energy density, for $\Lambda_e = 1, \epsilon = 0.01, \eta = 2.50$ and four different λ values. Solid black line represents the phantom divide, $\Pi/\rho = -4/3$. To better visualize the fluid evolution we have considered $\mathfrak{w} = 1.0$.

and $\eta > 1$. When λ is large and approaches unity, the fluid, whose evolution begins in an out-of-equilibrium state, initially evolves even farther away from equilibrium before ultimately achieving the equilibrium state in the later phase, as illustrated in all three figures. In certain instances, the fluid may even exit the acceptable regime and enter the phantom era where, $\Pi/(\rho + p) < -1$ (as is the case of olive curve in Fig. 4), before attaining equilibrium. While this kind of behavior implies the interesting scenario where the bulk viscous fluid crosses the phantom divide twice, such cases are plagued by causality violations. A similar case occurs when the values of η and ϵ are fixed, and λ is increased significantly (above unity). Here, it was observed that, at some finite energy density, viscous pressure diverges in the negative side, undergoes sign switching, and approaches zero from positive side, as seen from Fig. 4. As a result, this case also does not respect causality and should therefore be neglected.

In addition to pathological behaviors discussed above, which may only arise in certain regions of the parameter space, truncated generalized IS equation (19) also possess an unstable equilibrium point in Minkowski spacetime as shown in Appendix A. Assessing and resolving such instabilities is important, since relativistic dissipative hydrodynamics is locally governed by Minkowskian physics and instabilities in flat spacetime could persist even in cosmological backgrounds. In the present case, one can show that such an unstable equilibrium point exists at $\Pi_\star = -1/\lambda$. However, if we constrain the bulk viscous pressure within the limit $\Pi > -1/\lambda$, then the present case permits stable acceptable evolutionary behavior for the fluid within a bounded region of λ values. This can be seen as follows; if we initialize Π such that $\mathfrak{w} \lesssim 4/3$, we see that for $\Lambda_e = 1$ we will get $\Pi \lesssim -4/3$ and to satisfy the stability condition $\Pi > -1/\lambda$, we must constrain the nonlinear parameter within the limit, $0 \leq \lambda < 3/4$.

Hence, the simplest way to ensure viable solutions in this truncated nonlinear regime is to constrain the fluid parameters with the limit; $\epsilon \ll 1$, $0 \leq \lambda < 3/4$, and $\eta \geq 1$.

C. BISF in the full nonlinear regime

In the full nonlinear regime, the extended IS relation (13) becomes (for $n = 0$),

$$\frac{d\Pi}{d\rho} = \epsilon + \eta\left[\frac{\Pi e^{\lambda\Pi}}{\rho}\right]. \tag{24}$$

This ODE in general does not offer analytical solution, and therefore one must solve this numerically by employing suitable initial condition. In the present case we consider; $\Pi(\Lambda_e) = -\mathfrak{w}\Lambda_e$ at $\rho = \Lambda_e$ and then set $\Lambda_e = 1$. Sampling the parameter space of the model and solving the ODE numerically in each case, one can construct scatter and contour plots similar to those obtained in the previous cases. Doing this, we obtain all the plots provided in Figs. 5–7.

Looking at the Figs. 5(a) and 5(b), we infer that the BISF in the full nonlinear regime is guaranteed to evolve from a far-from-equilibrium state to a near-equilibrium regime with the dilution of energy density when $\eta > 1$, $\epsilon \ll 1$, and for both $\lambda > 0$ and $\lambda < 0$. At first glance, Fig. 5(b) might suggest that negative values of λ permit physically acceptable fluid evolution even when $\eta < 1$. However, a more careful examination of the contour plot obtained by slicing the 4D scatter plot 5(b) at $\eta = 0.50$ [see Fig. 6(b)] reveals that, even though the viscous fluid initially approaches equilibrium as the energy density decreases, it subsequently departs from equilibrium beyond a certain point. This feature is also evident in Fig. 7(b), where the evolution of Π/ρ is shown for $\lambda = -1$, $\epsilon = 0.01$, and $\mathfrak{w} = 1.00$ for different values of η. Notably, even when the fluid is initialized sufficiently away from the admissible upper bound ($\mathfrak{w} < 4/3$), it eventually evolves toward an out-of-equilibrium state as the energy density decreases. This behavior violates the acceptability criterion defined earlier. To obtain a physically viable evolution for the fluid in this case, one must therefore have $\eta > 1$.

Figures 5(a), 6(a), and 7(a) further show that viable fluid behavior at large values of λ demands correspondingly larger values of η. In such cases, the fluid evolves slowly while remaining far from equilibrium and subsequently undergoes rapid relaxation toward near equilibrium once the energy density becomes sufficiently small. Moreover, for sufficiently large values of λ, the fluid is driven even farther away from equilibrium, into the phantom regime, before approaching equilibrium, as illustrated in Figs. 6(a) and 7(a). Evidently, the crossing of the phantom divide appears to be a generic feature of both truncated and fully nonlinear regimes at large values of nonlinear coupling parameter. However, the pathological sign-switching behavior observed in the truncated case is absent in the

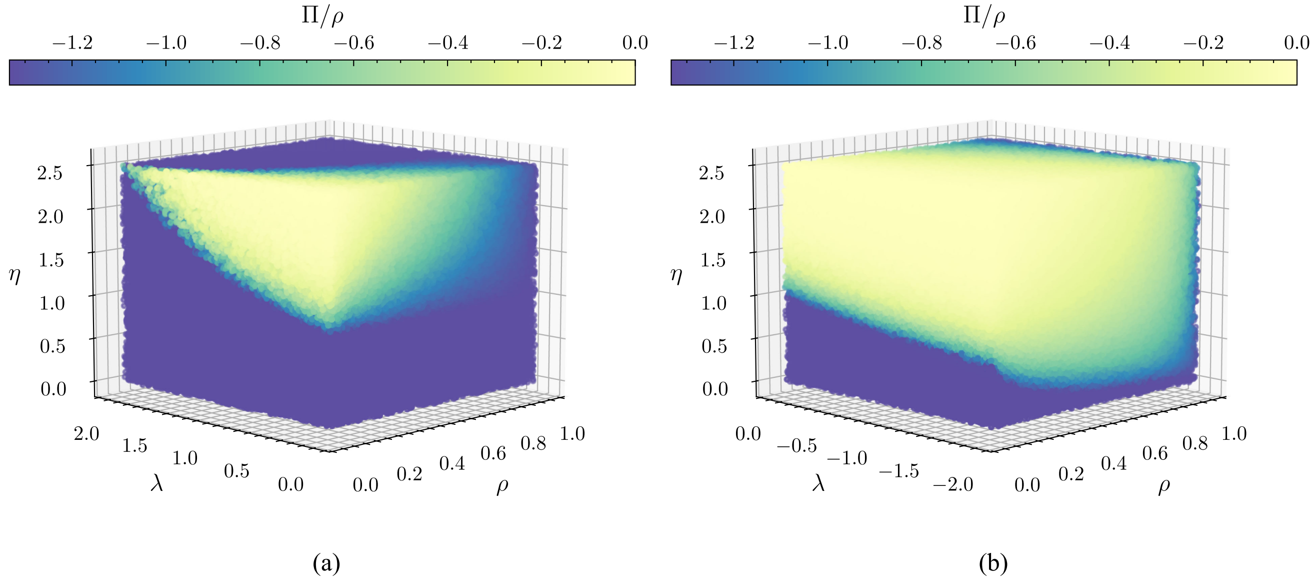

FIG. 5. 4D scatter plots illustrating the evolution of Π/ρ as a function of three parameters for $\epsilon = 0.01$ and $\mathfrak{w} = 1.33$ in the full nonlinear regime of a BISF. (a) $\epsilon = 0.01$ and $\lambda > 0$. (b) $\epsilon = 0.01$ and $\lambda < 0$.

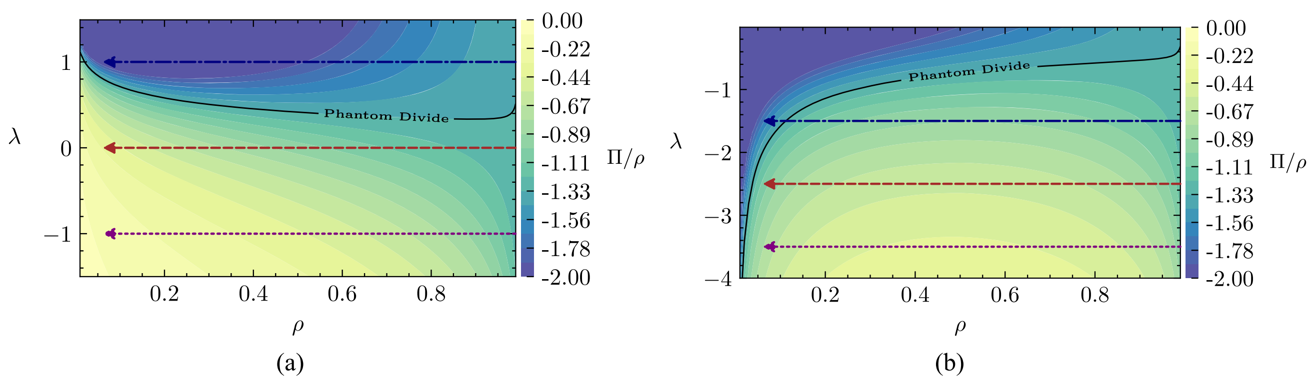

FIG. 6. These are contour plots showing the evolution of Π/ρ with ρ in the full nonlinear regime, for $\mathfrak{w} = 1.33$, $\epsilon = 0.01$ and two different η values. Phantom divide is depicted as a solid black line. (a) For $\eta = 1.50$. (b) For $\eta = 0.50$ and $\lambda < 0$.

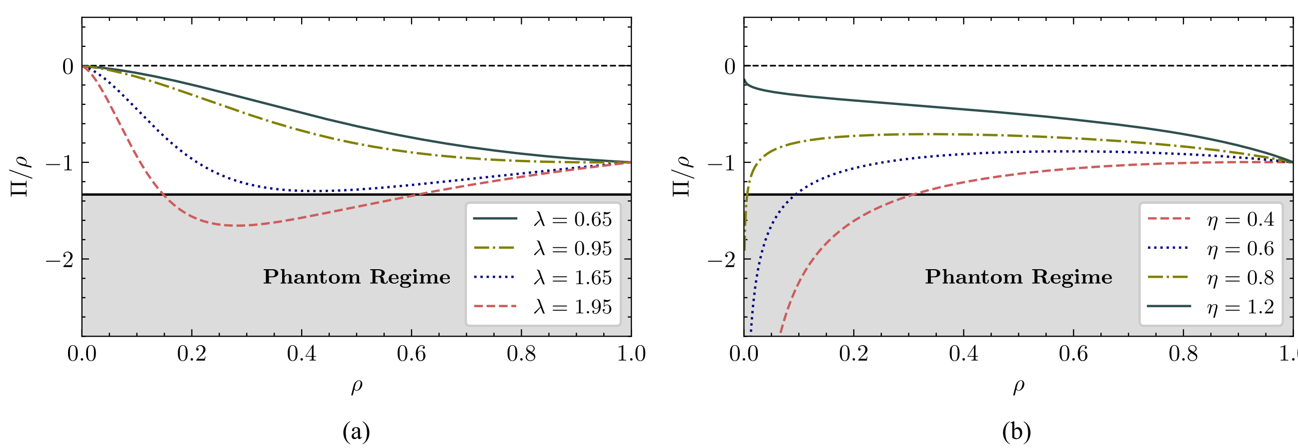

FIG. 7. Evolution of Π/ρ with ρ for $\mathfrak{w} = 1.00$, $\epsilon = 0.01$ and different values of η and λ in the full nonlinear regime. (a) For $\eta = 2.50$ and different λ. (b) For $\lambda = -1.0$ and different η.

fully nonlinear scenario. Additionally, the IS equation in the full nonlinear regime, i.e., Eq. (5) admits only a single stable fixed point in Minkowski spacetime and is therefore free from the instabilities encountered in the previous case (see Appendix A). This implies that, unlike the truncated regime, the fully nonlinear framework does not impose stringent theoretical bounds on the nonlinear coupling parameter λ.

In the full non-linear regime, viable solutions require: $\epsilon \ll 1$, $\eta \geq 1$ with both, $0 < \lambda \ll 1$, and $\lambda \leq 0$.

IV. DYNAMICAL SYSTEM ANALYSIS OF THE COUPLED EINSTEIN-ISRAEL-STEWART SYSTEM IN THE FULL NONLINEAR REGIME

Evolution of bulk viscous fluid and the expansion of the Universe can be studied by solving the Israel-Stewart equation (5), which is coupled to the Einstein equations via the continuity relation (2). These two expressions together form the coupled Einstein-Israel-Stewart system (EIS). By recasting these equations in terms of the dimensionless variables $\Omega_\rho = \rho/\Lambda_e$ and $\Omega_\Pi = \Pi/\Lambda_e$, we obtain the 2D nonlinear autonomous system,

$$\Omega_\rho' = -3[(1 + w_0)\Omega_\rho + \Omega_\Pi], \tag{25}$$

$$\Omega_\Pi' = \Omega_\rho' \left\{ \epsilon + \eta \left[\frac{\Omega_\Pi e^{\tilde{\lambda}\Omega_\Pi}}{\Omega_\rho} \right] \right\}. \tag{26}$$

Here, we have denoted $\tilde{\lambda} = \lambda\Lambda_e$ and overhead "*prime*" signifies derivative with respect to the number of e-folds N, which is defined as $N = \ln(a/a_i)$, with "a_i" being scale factor at the beginning (which we set to 1), and "a" is the scale factor at some later time.

Even though the dynamical variables $(\Omega_\rho, \Omega_\Pi)$ provide a convenient representation of the system in terms of bulk energy density and viscous pressure, the resulting 2D autonomous system defined by Eqs. (25) and (26) becomes singular at $\Omega_\rho = 0$ due to the appearance of Ω_ρ in the denominator of Eq. (26). As a result, the fixed point $(\Omega_\rho, \Omega_\Pi) = (0, 0)$ becomes ill defined unless a physically motivated limiting condition is imposed on the system that can ensure that the ratio Π/ρ remains finite as $\rho \to 0$. Physically, such a condition can arise from the expectation that, in the late phase of the universe, the dissipative fluid approaches its near-equilibrium state. In this regime, the bulk viscous pressure should at least scale in proportion with the energy density, i.e., $\Pi/\rho \to -\kappa$, where κ is a finite constant. From the result that we have derived in the linear near-equilibrium regime, i.e., Eq. (17), one can confirm that this is indeed true. By this consideration, it is natural to reformulate the phase space in terms of the ratio Π/ρ, rather than Π, which will then remove the singular behavior at vanishing energy density and allow us to perform a well-defined stability analysis. Accordingly, we introduce the phase-space variables,

$$x = \Omega_\rho \quad ; \quad y = \Pi/\rho = \Omega_\Pi/\Omega_\rho. \tag{27}$$

Note that this change of variables does not modify the physical content of the EIS equations, but only provides a well-defined representation of the autonomous system for better analyzing the stability of fixed points. In terms of the new variables (x, y) defined above, we can rewrite the 2D autonomous system in Eqs. (25) and (26) as follows;

$$x' = f = -3x[1 + w_0 + y], \tag{28}$$

$$y' = g = -3[1 + w_0 + y]\{\epsilon + y[\eta e^{\tilde{\lambda}xy} - 1]\}. \tag{29}$$

Importantly, notice that in the above formulation, the EIS system remains regular at $x = 0$. This autonomous set of equations admits (a) isolated fixed point "P" at which $x = 0$ and $y = \epsilon/(1 - \eta)$ and (b) a line of fixed points "L" along which $y = -(1 + w_0)$. Notably, at the fixed point where the energy density vanishes, y attains the same finite value as obtained in the linear regime of IS equations when fluid nears its equilibrium state, i.e., Eq. (17). Furthermore, one should also keep in mind that, the line of equilibrium points "L" corresponds to regimes where the fluid is far from equilibrium, and therefore if one expects the fluid to evolve from a far-from-equilibrium state in the early Universe to a stable equilibrium state in the late phase, then L must be a line of unstable equilibrium points, and P must be a stable fixed point.

To determine the nature of fixed points, we construct the Jacobin matrix ($\mathcal{J}$) of the autonomous system (28) and (29) and then determine its eigenvalues. For the system that we are considering, $\mathcal{J}$ is defined as,

$$\mathcal{J} = \begin{bmatrix} \partial_x f & \partial_y f \\ \partial_x g & \partial_y g \end{bmatrix} \tag{30}$$

and by using Eqs. (28) and (29) we get,

$$\partial_x f = -3(1 + w_0 + y) \quad ; \quad \partial_y f = -3x \tag{31}$$

$$\partial_x g = -3(1 + w_0 + y)\tilde{\lambda}\eta y^2 e^{\tilde{\lambda}xy} \tag{32}$$

$$\begin{aligned} \partial_y g = &-3(1 + w_0 + y)\{\eta e^{\tilde{\lambda}xy}[1 + \tilde{\lambda}xy] - 1\} \\ &- 3\{\epsilon + y[\eta e^{\tilde{\lambda}xy} - 1]\}. \end{aligned} \tag{33}$$

To analyze the stability of the system near the fixed points, we only need to determine the nature of eigenvalues of $\mathcal{J}$ at those fixed points. We do this as follows:

(a) *Isolated fixed point* "P": Here, the fixed point occurs at, $(x, y) = (0, \kappa)$, where $\kappa = \epsilon/(1 - \eta)$. At this fixed point the Jacobian can be simplified to form a 2D triangular matrix with one of-diagonal element going to zero (i.e., $\partial_y f|_{x=0} = 0$). This means, the eigenvalues of the Jacobian matrix at "P" are just the diagonal elements evaluated at "P," given as,

$$\chi_P^{(i)} = -3[1 + w_0 + \epsilon/(1-\eta)], \tag{34}$$

$$\chi_P^{(j)} = -3[1 + w_0 + \epsilon/(1-\eta)](\eta - 1). \tag{35}$$

From the above equations, we find that the eigenvalues at P are real numbers that are guaranteed to be negative if $\eta > 1$ and $|\epsilon/(1-\eta)| \ll 1$, indicating linear stability of this point. This means, small perturbations from this equilibrium solution decay with time and approach the fixed point P in an monotonic fashion, and the EIS system is driven toward P at late times. It is interesting to note that late-time stability of the system is independent of the value of nonlinear parameter λ, and depends only on the model parameters governing the evolution of the fluid in the near-equilibrium state, i.e., (w_0, η, ϵ).

Therefore, P represents a stable late-time attractor of the EIS system, corresponding to the relaxation of BISF toward the near-equilibrium state as energy density dilutes. Note that this is true only if the ratio Π/ρ remains finite, or vanishes altogether in the late phase. This is exactly the condition that one requires for having a physically acceptable hydrodynamic behavior, i.e., the bulk viscous fluid retains its near-equilibrium state, as the coupled EIS system evolves toward its stable late-time fixed point.

(b) *Line of fixed points* "L": At the line of fixed points "L" we have $y = -(1 + w_0)$. Consequently, among the four terms in the Jacobian, i.e., Eqs. (31)–(33), only the second equation in (31), and the second term in Eq. (33) survive. Therefore, the determinant of the resulting Jacobian at the line of fixed point vanishes, which in turn results in the vanishing of one of its eigenvalues. The stability of the system near the line of fixed points is then determined by the sign of the remaining eigenvalue, which is simply the trace of the Jacobian itself, given by the expression,

$$\chi_L = -3\{\epsilon + (1 + w_0)[1 - \eta e^{-\tilde{\lambda}(1+w_0)\Omega_\rho}]\}. \tag{36}$$

Note that the eigenvalue χ_L can assume both positive and negative values depending on the model parameters. To examine the stability of the line of fixed points, we evaluate χ_L for $w_0 = 1/3$ and $\Omega_\rho = 1$, and display its behavior in the Figs. 8(a) and 8(b), according to which, we observe that χ_L becomes positive in the region $\lambda \ll 1$ and $\eta > 1$ when $\epsilon = 0.01$. However, when $\epsilon = 2/3$, the instability region shifts toward larger values of η, with $\chi_L > 0$ typically requiring $\eta \gtrsim 1.5$ for $\lambda \ll 1$. This indicates that larger ϵ values can suppress the instability introduced by weak nonlinear coupling and reduce the parameter space that admits unstable fixed points. In the regime of negative nonlinear coupling ($\lambda < 0$), the line of fixed points can become unstable for any $\eta > 1$, provided that λ is sufficiently negative. The degree of negativity required for λ increases with ϵ. In particular, when $\epsilon = 2/3$, small negative values of λ are insufficient to render the line of fixed points to be unstable. Instead, large negative values of λ are required to ensure $\chi_L > 0$.

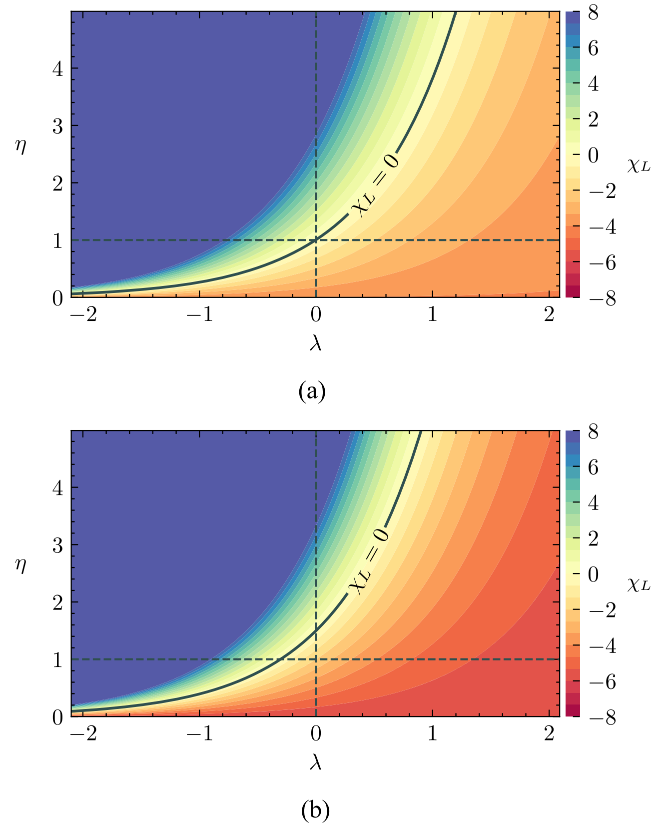

FIG. 8. Plot of the eigenvalue χ_L that determines the stability of the system at the line of fixed points "L." Parameter spaces offering unstable fixed points are the ones with positive χ_L values, i.e., yellow → blue region. (a) $\epsilon = 0.01$. (b) $\epsilon = 2/3$.

The region of parameter space where we have $\chi_L < 0$ may correspond to attractorlike behavior. However, a rigorous assessment of stability in this regime requires a center manifold analysis. However, if one adopts the physical expectation that the EIS system should exhibit an unstable fixed point when the dissipative fluid is far from equilibrium, then it is sufficient to restrict the parameter space to the regime $\lambda \ll 1$, $\eta > 1$, and $\epsilon \ll 1$, (note that $\lambda < 0$ is also allowed).[3] This particular region of parameter space can offer unstable early time fixed points, which in

[3]To determine the parameter space where L becomes unstable, a center manifold analysis is not necessary. Presence of a positive nonzero eigenvalue is sufficient to establish instability [37].

turn allows the universe to evolve away from an early time viscous driven quasi–de Sitter phase and evolve toward the stable fixed point P at late times. However, since the sign of χ_L depends on the precise values of the model parameters, which are generally correlated, ensuring the instability of the line of fixed points requires imposing the inequality constraint $\chi_L > 0$, expressed in terms of model parameters using Eq. (36) as given below (recall that we have initialized $\Lambda_e = 1$),

$$\lambda < \frac{1}{1+w_0} \ln\left\{\frac{\eta(1+w_0)}{1+w_0+\epsilon}\right\}. \tag{37}$$

Fixing the values, $w_0 = 1/3$, $\epsilon \ll 1$, we can get an upper bound on nonlinear parameter λ as $\lambda < 3\ln(\eta)/4$. This inequality constraint can guarantee that $\chi_L > 0$ and should therefore be imposed in numerical investigations, while comparing the model with observational data.

A. Slow-roll expansion driven by viscous cosmic fluid

Considering the cosmic fluid in the early Universe to be in a far from equilibrium state ($|\Pi| \approx \rho + p$), and the EIS system to be initialized very close to the unstable fixed point, we numerically solve the coupled Eqs. (25) and (26) by adopting a set of parameter values in the unstable region in the plot 8(a) where $\chi_L > 0$. Then by using the obtained solution, we study the evolution characteristics of the Hubble parameter of the universe and its derivatives.

In the far from equilibrium regime, the bulk viscosity associated with the effective cosmic fluid can be large enough to cause a violation of one of the strong energy conditions, i.e., $\rho + 3p > 0$, for a very small time and hence cause an accelerated expansion of the universe for a brief period. This can be visualized from the plot of deceleration parameter "q" depicted in Fig. 9. There, we have expressed q in terms of the number of e-folds "$N = \ln(a)$" as, $q = -(1 + d\ln(H)/dN)$. An e-fold (N) is the time interval during which the scale factor $a(t)$ of the Universe increases by a factor of "e" ($\approx$2.718).

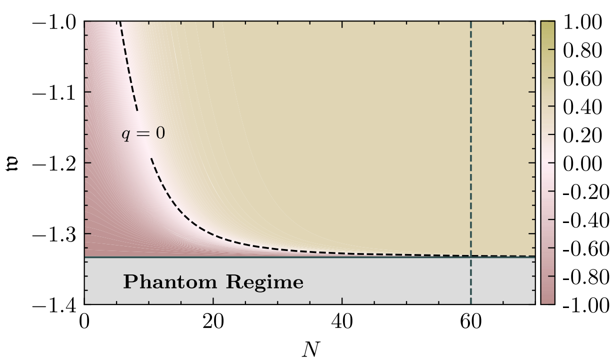

FIG. 9. Contour plot of deceleration parameter with number of e-folds "N" for different values of $\mathfrak{w}$ in the full nonlinear regime. For better visualization of the early transition point, we have considered the values $\epsilon = 0.035$, $l = 0.05$ $\eta = 1.10$, $w_0 = 1/3 \Rightarrow \chi_L = 0.01$.

As the fluid relaxes from its initial out-of-equilibrium phase in the early Universe to stable equilibrium in the late phase, the Universe transitions from an accelerated to decelerated expansion phase. Furthermore, the exact transition point and the time interval of this accelerating phase depends on both, the value of model parameters, and the initial conditions applied on the model. Also, to produce a quasi–de Sitter expansion driven by a viscous fluid having $c_s^2 = w_0 = 1/3$, the initial conditions must be such that the value of the nonequilibrium parameter "$\mathfrak{w}$" is close to 4/3. In addition to this, in Fig. 9 we also see that in the case where $\epsilon = 0.035$, $\eta = 1.10$, $\lambda = 0.05$, and $w_0 = 1/3$, the value of nonequilibrium parameter $\mathfrak{w}$ must tend to 4/3 for sustaining an accelerated expansion that spans 50 e-folds or greater. Hence, as $\mathfrak{w} \approx 4/3$, (a) the duration of the early accelerated expansion will be longer, and (b) it will more closely resemble the de Sitter phase.

The dynamics of the early Universe, in particular the inflationary background, is better characterized using the Hubble slow-roll parameters, which forms a hierarchy, and is defined as the successive derivatives of the Hubble parameter with respect to the number of e-folds,

$$\epsilon_{n+1} \equiv \frac{d\,\ln|\epsilon_n|}{dN}, \tag{38}$$

with the first one defined as, $\epsilon_1 \equiv -\dot{H}/H^2$. These model independent parameters are significant as they directly determine the value of cosmological observables such as the scalar spectral tilt (n_s) and its running (α_s) [38,39]. To solve the coupled EIS system we consider,[4] $\epsilon = 0.01$, $\eta = 1.50$, $w_0 = 1/3$, $\lambda = 0.2975$ along with the initial condition, $\mathfrak{w} = 1.333$ with $\Lambda_e = 1$, and investigate the cosmological dynamics in the early Universe. Note that this sample set of parameter values leads to $\chi_L = 0.005$, which guarantees an unstable fixed point in the early Universe, and predicts a "50 − e-fold" inflationary scenario.

The evolution of ϵ_1, ϵ_2, and ϵ_3 with the number of e-folds for acceptable values of free parameters mentioned earlier, is provided in Fig. 10. In addition to this, we have also plotted the evolution of deceleration parameter "q" and the near-equilibrium condition $\Pi/(\rho + p)$, to better asses the evolution of the viscous fluid in conjunction with expansion of the Universe. Clearly, the parameter ϵ_1 remains well below unity until $N \approx 50$, confirming a background evolution that is deep in the accelerating regime. Then, its subsequent monotonic rise with the number of e-folds indicates a gradual approach toward the end of inflation. Notably, in Fig. 10 we also infer that the dissipative cosmic fluid is indeed evolving toward equilibrium as the Universe

[4] We choose this particular set of parameter values because they predict an accelerated expansion era that spans 50 e-folds.

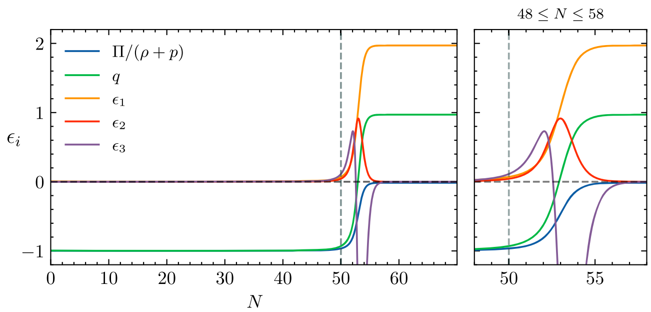

FIG. 10. Evolution of Hubble slow-roll parameters for, $\epsilon = 0.01$, $\eta = 1.50$, $w_0 = 1/3$, $\lambda = 0.2975$, and $\mathfrak{w} = 1.333$.

expands, i.e., $|\Pi|/(\rho + p)$ decreases with increase in N. The higher-order parameters ϵ_2 and ϵ_3 exhibit no particular oscillations/fluctuations around zero and therefore do not introduce unwanted instabilities. Hence, the scalar spectral tilt remains stable over the observable window, which can therefore yield predictions consistent with the Planck 2018 constraints [40]. Furthermore, the smallness of ϵ_3 implies that the running of the spectral index is naturally negligible, which is also in agreement with current upper limits. The absence of abrupt jumps or sign-changing excursions in ϵ_2 and ϵ_3 indicates a smooth evolution that is free from transient dynamical effects such as steps and turns. Overall, the present model provides a coherent, observationally viable slow-roll trajectory, equivalent to a stable single-field inflation and consistent with CMB constraints [40]. Finally, the evolution in Fig. 10 clearly shows that ϵ_1 rises smoothly from its inflationary value $\epsilon_1 \ll 1$, reaches the end-of-inflation condition $\epsilon_1 = 1$, and then approaches $\epsilon_1 = 2$. This final value corresponds to a radiation-dominated Universe with equation of state $\omega = 1/3$. Thus, the model provides a smooth and natural transition from inflation to radiation domination, which is consistent with the expected thermal history of the early Universe.

Similar evolutionary behaviors for the Universe are also possible in truncated EIS equations within the acceptable region of parameter space determined in Sec. III B; we have provided a detailed analysis in Appendix D.

V. RESULTS AND CONCLUSION

In this work, we derived a generalized expression for the relaxation time of a BISF by using the nonlinear causality constraint, and examined its dynamical consequences in an extended fully nonlinear version of the IS equation with an explicit exponential nonlinear dissipative term. This particular extension of the IS equation incorporates higher order viscous corrections within the exponential functional form and therefore remains valid when fluid goes arbitrarily far from equilibrium. A central outcome of adopting the causal relaxation time is that the nonlinear Israel-Stewart evolution equation reduces to a first-order nonlinear differential relation connecting the bulk viscous pressure and the energy density. Remarkably, this relation holds in any homogeneous and isotropic spacetime. Furthermore, since the relaxation time is fixed directly by the causality requirement, the resulting formulation guarantees causal evolution even in regimes far from equilibrium. As a result, dynamical description of dissipative fluids becomes significantly simplified without sacrificing the causal structure.

When applied to a spatially flat FLRW background, this formulation of the IS equation admits new class of exact analytical solutions for BISF in both linear and certain truncated nonlinear regimes. These solutions then lead to an effective equation of state exhibiting a generalized polytropic form, which is often adopted phenomenologically in the literature. A dynamical systems analysis of the coupled EIS equations was performed, which revealed that the dynamical system contains a line of unstable fixed points and a stable late-time attractor. This structure allows the cosmological evolution to originate from an early far-from-equilibrium phase and subsequently relax toward equilibrium at late times. We further show that the present framework can support an observationally consistent transient viscous-driven slow-roll expansion that smoothly exits into a radiation-dominated epoch, a feature that is difficult to realize within standard inflationary scenarios. Moreover, under the parameter constraints derived in this work, the EIS system exhibits an intuitive and physically consistent hydrodynamic evolution, wherein the fluid evolves from a far-from-equilibrium state to a near-equilibrium state as the dynamical system transitions from an unstable early-time fixed point to the stable late-time attractor.

Beyond the specific cosmological scenario considered here, the formalism developed in this work provides a flexible framework for constructing a broad class of inflationary models and for investigating dissipative dynamics in relativistic systems. In the context of early-universe cosmology, the causal relaxation time introduced here may enable a more realistic description of viscous effects and particle production during the quark-gluon plasma epoch and the reheating phase. In astrophysical settings, the extended relaxation-time formulation may improve the modeling of bulk-viscous damping, thermalization, and other far-from-equilibrium processes in neutron-star interiors, proto-neutron–star evolution, and postmerger dynamics, where significant departures from equilibrium are expected [41–45]. Since the form of relaxation time is determined *a priori* by the causality constraint, the exact formulation of IS equations requires fewer phenomenological assumptions and therefore becomes more robust. For this reason, the framework presented here is especially well suited for studying far-from-equilibrium regimes, where the choice of dissipative variables and transport coefficients becomes ambiguous.

ACKNOWLEDGMENTS

We thank the reviewers for their insightful comments, which significantly improved our manuscript. V. A. P. thanks Cochin University of Science and Technology for providing the financial support in the form of Senior Research Fellowship. The authors acknowledge the assistance of Grammarly in improving the grammar and language usage in this article.

DATA AVAILABILITY

The data that support the findings of this article are not publicly available. The data are available from the authors upon reasonable request.

APPENDIX A: STABILITY OF TRUNCATED AND FULLY NONLINEAR ISRAEL-STEWART EQUATION IN MINKOWSKI SPACETIME

In Minkowski spacetime we have $\nabla_\mu u^\mu = 0$, in this limit the nonlinear Israel-Stewart equation (5) exactly reduces to the autonomous first-order ODE,

$$\dot{\Pi} = -\frac{1}{\tau_\Pi}\Pi e^{\lambda\Pi}, \tag{A1}$$

where the relaxation time τ_Π is allowed to depend also on Π. Equation (A1) represents a nonlinear relaxation law with a fixed point solution, $\Pi_\star = 0$. Evidently, no additional stationary solution exists. Since Eq. (A1) defines a one-dimensional autonomous dynamical system of the form, $\dot{\Pi} = f(\Pi)$, the linear stability of the fixed point $\Pi_\star$ is determined solely by the sign of the derivative $f'(\Pi_\star)$, where "*prime*" denotes derivative with respect to Π. Differentiating $f(\Pi)$ with respect to Π, we obtain,

$$f'(\Pi) = \frac{e^{\lambda\Pi}}{\tau_\Pi}\left[\Pi\frac{\tau'_\Pi}{\tau_\Pi} - (1+\lambda\Pi)\right]. \tag{A2}$$

Evaluating this expression at the fixed point $\Pi_\star = 0$, we obtain the equation,

$$f'(\Pi_\star) = f'(0) = -\frac{1}{\tau_\Pi(0)}. \tag{A3}$$

Since the relaxation time at equilibrium state should be positive, $\tau_\Pi(0) > 0$, we have $f'(0) < 0$ irrespective of the value of λ. Therefore, in the full nonlinear regime, the equilibrium solution becomes asymptotically stable.

Truncated nonlinear case: If we truncate the nonlinear IS equation given in Eq. (5), by considering only up to second power of Π, in Minkowski spacetime we obtain the ODE of the form;

$$\dot{\Pi} = -\frac{1}{\tau_\Pi}\Pi(1+\lambda\Pi). \tag{A4}$$

Here, we see that there can be two equilibrium points, one at, $\Pi^a_\star = 0$ and other one at $\Pi^b_\star = -1/\lambda$. To determine the stability we consider the same approach as in the previous case. Here, $f'(\Pi)$ becomes,

$$f'(\Pi) = \Pi(1+\lambda\Pi)\frac{\tau'_\Pi}{\tau^2_\Pi} - \frac{1}{\tau_\Pi}(1+2\lambda\Pi). \tag{A5}$$

(i) For the equilibrium solution $\Pi^a_\star = 0$, we once again obtain a stable point, since $f'(0) = -1/\tau_\Pi(0)$ and $\tau_\Pi(0) > 0$ at all times.

(ii) For the second equilibrium point $\Pi^b_\star = -1/\lambda$, we see that $f'(\Pi^b_\star) = 1/\tau_\Pi(\Pi^b_\star)$, which has a positive definite value at all times. Consequently, this is an unstable fixed point of the system. As a result, the viable solutions that converge to $\Pi = 0$ are obtained only within the limit, $\Pi > -1/\lambda$.

APPENDIX B: DERIVING THE EXPRESSION FOR CAUSAL RELAXATION TIME

The causality constraint derived in [19] is given by

$$\left[\frac{\zeta_\Pi}{\tau_\Pi} + \mathfrak{n}\omega_\mathfrak{n}\right]\frac{1}{\rho+p+\Pi} + \omega_\rho \le 1, \tag{B1}$$

where $\omega_\mathfrak{n} = \partial p/\partial\mathfrak{n}$ and $\omega_\rho = \partial p/\partial\rho$. The left-hand side of Eq. (B1) represents the effective squared speed of sound in the dissipative medium, c^2_{acoustic} [19]. The above inequality therefore ensures that the total signal propagation speed does not exceed the speed of light. For a barotropic fluid having, $\omega_\mathfrak{n} = 0$ and $\omega_\rho = w_0$, Eq. (B1) reduces to,

$$c^2_{\text{acoustic}} = c^2_s + c^2_b \le c^2, \tag{B2}$$

where

$$c^2_s = w_0 c^2 \quad ; \quad c^2_b = \frac{\zeta_\Pi}{\tau_\Pi(\rho+p+\Pi)}c^2. \tag{B3}$$

Here, we have denoted "c_s" as the adiabatic speed of sound, while "c_b" represents the propagation speed of bulk viscous perturbations.

In causal relativistic thermodynamics, the relaxation time τ_Π ensures that dissipative signals propagate with finite speed, thereby removing the acausal behavior present in first-order theories. As discussed by Maartens [24], the ratio "ζ_Π/τ_Π" may be governed by microscopic transport processes such as interaction times and mean free paths, and can hence determine the characteristic propagation speed of bulk viscous stresses. Using the above definitions, the causality condition becomes,

$$\frac{c_b^2}{(1-w_0)c^2} \le 1. \tag{B4}$$

If we therefore define the dimensionless parameter,

$$\epsilon_0 \equiv \frac{c_b^2}{(1-w_0)c^2}, \tag{B5}$$

then, the expression for relaxation time of the fluid is exactly given by the relation,

$$\tau_\Pi = \frac{\zeta_\Pi}{\epsilon_0(1-w_0)(\rho+p+\Pi)}. \tag{B6}$$

This is a physically motivated causality based expression for the relaxation time of the viscous fluid. The constant parameter ϵ_0 measures how strongly viscous disturbances contribute to the total signal propagation speed in the fluid. Very small values of ϵ_0 indicate that bulk viscous perturbations propagate slowly, whereas values of ϵ_0 close to unity imply that viscous signals propagate close to the maximum speed allowed by causality.

APPENDIX C: VISCOELASTIC AND PSEUDOPLASTIC REGIMES OF FULLY NONLINEAR ISRAEL-STEWART THEORY

According to relativistic bulk rheology framework of [46], a pseudoplastic fluid is described as the one whose effective bulk viscosity can be expressed as the function of expansion rate, i.e., $\Pi = -f(\theta)$, while viscoelastic fluids evolve dynamics in which the evolution of bulk viscosity follows a relaxation type equation, leading to time-dependent stress response even for fixed expansion rate, i.e., $\tau\dot{\Pi} + \Pi = -\zeta\theta$. Here, our aim is to analyze these behaviors for the fully nonlinear Israel-Stewart equation proposed in this article.

Viscoelastic regime: When the bulk viscous pressure becomes relatively small and close to zero, i.e., $|\lambda\Pi| \ll 1$, the exponential relation can be Taylor expanded as,

$$\Pi e^{\lambda\Pi} \simeq \Pi + \lambda\Pi^2 + \frac{\lambda^2}{2!}\Pi^3 + \cdots, \tag{C1}$$

and as a result, Eq. (5) reduces to,

$$\tau_\Pi u^\mu \nabla_\mu \Pi + \Pi \simeq -\zeta\theta. \tag{C2}$$

This is precisely the causal relaxation equation of the Israel-Stewart type, in which Π relaxes toward the Navier-Stokes value on a finite timescale τ_Π. Hence, the dynamics in this scenario is analogous to a viscoelastic fluid, in which stress relaxes over a characteristic time and displays combined viscous and elastic features.

Pseudoplastic regime: To investigate the possibility of a pseudoplastic behavior, we must consider the quasistationary limit where $|u^\mu\nabla_\mu\Pi| \approx 0$ and τ_Π has a small and finite value. With this approximation, the evolution equation (5) yields the algebraic relationship

$$\Pi e^{\lambda\Pi} = -\zeta\theta. \tag{C3}$$

This relation can be inverted using "Lambert *W function*" to obtain the bulk viscous pressure as,

$$\Pi = \frac{1}{\lambda} W(-\lambda\zeta\theta). \tag{C4}$$

In the small theta limit, $|\lambda\zeta\theta| \ll 1$, one finds

$$\begin{aligned}\Pi &\simeq \frac{1}{\lambda}\left\{-\lambda\zeta\theta - (\lambda\zeta\theta)^2 + \frac{3}{2}(\lambda\zeta\theta)^3 + \mathcal{O}[(\lambda\zeta\theta)^4]\right\} \\ &\simeq -\zeta\theta - \lambda\zeta^2\theta^2 + \frac{3}{2}\lambda^2\zeta^3\theta^3 + \mathcal{O}(\theta^4)\cdot\cdot \end{aligned} \tag{C5}$$

To leading order, the standard relativistic Navier-Stokes relation $\Pi \simeq -\zeta\theta$ is recovered, while higher-order terms encode nonlinear pseudoplastic corrections.

APPENDIX D: STABILITY ANALYSIS AND SLOW-ROLL EXPANSION IN THE TRUNCATED NON-LINEAR REGIME

For truncated nonlinear BISF considered in Sec. III B, the coupled EIS equations become,

$$\Omega_\rho' = -3[(1+w_0)\Omega_\rho + \Omega_\Pi], \tag{D1}$$

$$\Omega_\Pi' = \Omega_\rho'\left\{\epsilon + \eta[1-\tilde{\lambda}\Omega_\Pi]\frac{\Omega_\Pi}{\Omega_\rho}\right\}. \tag{D2}$$

We can express this equation in terms of the dynamical variables, $x = \Omega_\rho$ and $y = \Omega_\Pi/\Omega_\rho$ as;

$$x' = -3x[1+w_0+y], \tag{D3}$$

$$y' = -3[1+w_0+y]\{\epsilon + y[\eta(1-\tilde{\lambda}xy)-1]\}. \tag{D4}$$

This 2D autonomous system, like the full nonlinear case, has an isolated fixed point, $(x,y) = (0, \epsilon/(1-\eta))$ and the line of fixed points $y = -(1+w_0)$. If we then determine the Jacobian matrix at the isolated fixed point and derive the eigenvalues at that point, we will indeed obtain the same result as in the full nonlinear regime. That is, the isolated fixed point becomes stable if $\eta > 1$ and $|\epsilon/(1-\eta)| \ll 1$. This is indeed because of the fact that the eigenvalue of the Jacobian at this point is independent of λ. Parameter spaces offering an unstable fixed point at the line are then determined by the sign of the nonzero eigenvalue;

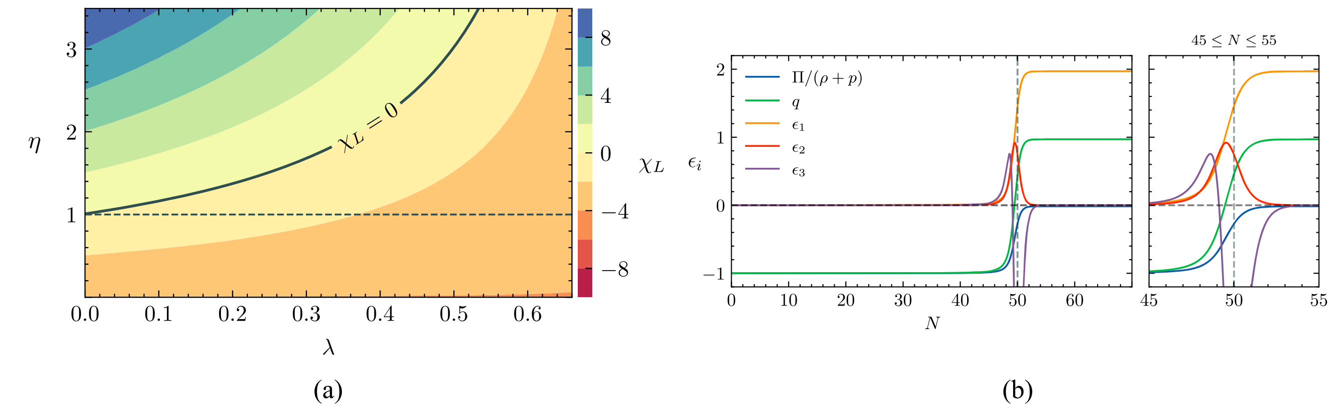

FIG. 11. Numerical plots associated with BISF in the truncated nonlinear regime. (a) Contour plot of eigenvalue χ_L with $\epsilon = 0.01$. (b) Evolution of Hubble slow-roll parameters for truncated nonlinear BISF with $\epsilon = 0.01$, $\lambda = 0.2462$, $\eta = 1.50$, $w_0 = 1/3$, and $\mathfrak{w} = 1.333 \Rightarrow \chi_L = 0.004$.

$$\chi_L = -3\{\epsilon + (1 + w_0)[1 - \eta(1 - \lambda(1 + w_0)x)]\}. \tag{D5}$$

A contour plot of this expression is shown in Fig. 11(a). The figure indicates that the line of fixed points becomes unstable for $\eta > 1$ in the regime $\lambda \ll 1$ and $\epsilon \ll 1$. In this limit, one obtains an upper bound on λ, slightly different from the one obtained in the full nonlinear case, namely $\lambda < 3(\eta - 1)/(4\eta)$. Numerical solutions of the ODEs (D1) and (D2), illustrated in Fig. 11(b), demonstrate that the resulting cosmological evolution is dynamically equivalent to the full nonlinear regime.

[1] G. S. Rocha, D. Wagner, G. S. Denicol, J. Noronha, and D. H. Rischke, Entropy **26**, 189 (2024).
[2] M. Chabanov, L. Rezzolla, and D. H. Rischke, Mon. Not. R. Astron. Soc. **505**, 5910 (2021).
[3] P. Romatschke and U. Romatschke, *Relativistic Fluid Dynamics In and Out of Equilibrium*, Cambridge Monographs on Mathematical Physics (Cambridge University Press, Cambridge, England, 2019).
[4] R. Maartens, Classical Quantum Gravity **12**, 1455 (1995).
[5] W. Zimdahl, Phys. Rev. D **53**, 5483 (1996).
[6] C. Ganguly and J. Quintin, Phys. Rev. D **105**, 023532 (2022).
[7] J. A. S. Lima and A. S. M. Germano, Phys. Lett. A **170**, 373 (1992).
[8] W. Zimdahl, Mon. Not. R. Astron. Soc. **280**, 1239 (1996).
[9] N. Udey and W. Israel, Mon. Not. R. Astron. Soc. **199**, 1137 (1982).
[10] M. Giovannini, Phys. Rev. D **60**, 123511 (1999).
[11] J. P. Mimoso, A. Nunes, and D. Pavón, Phys. Rev. D **73**, 023502 (2006).
[12] N. Cruz, A. Hernández-Almada, and O. Cornejo-Pérez, Phys. Rev. D **100**, 083524 (2019).
[13] A. Sasidharan and T. K. Mathew, Eur. Phys. J. C **75**, 348 (2015).
[14] C. Eckart, Phys. Rev. **58**, 919 (1940).
[15] L. D. Landau and E. M. Lifshitz, *Fluid Mechanics* (Pergamon Press, New York, 1987).
[16] W. Israel and J. M. Stewart, Ann. Phys. (N.Y.) **118**, 341 (1979).
[17] W. A. Hiscock and L. Lindblom, Phys. Rev. D **31**, 725 (1985).
[18] W. Israel, Ann. Phys. (N.Y.) **100**, 310 (1976).
[19] F. S. Bemfica, M. M. Disconzi, and J. Noronha, Phys. Rev. Lett. **122**, 221602 (2019).
[20] L. Gavassino, Phys. Rev. D **111**, 083014 (2025).
[21] S. Weinberg, Astrophys. J. **168**, 175 (1971).
[22] G. L. Murphy, Phys. Rev. D **8**, 4231 (1973).
[23] N. Udey and W. Israel, Mon. Not. R. Astron. Soc. **199**, 1137 (1982).
[24] R. Maartens, arXiv:astro-ph/9609119.
[25] G. M. Kremer, Phys. Rev. D **68**, 123507 (2003).
[26] J. Peralta-Ramos and E. Calzetta, Phys. Rev. D **86**, 125024 (2012).
[27] J. D. Barrow, Phys. Lett. B **235**, 40 (1990).
[28] A. Kamenshchik, U. Moschella, and V. Pasquier, Phys. Lett. B **511**, 265 (2001).
[29] S. D. Campo and J. R. Villanueva, Int. J. Mod. Phys. D **18**, 2007 (2009).
[30] S. Nojiri, S. D. Odintsov, and S. Tsujikawa, Phys. Rev. D **71**, 063004 (2005).
[31] P. K. Dunsby, O. Luongo, M. Muccino, and V. Pillay, Phys. Dark Universe **46**, 101563 (2024).
[32] P.-H. Chavanis, J. Phys. Conf. Ser. **1030**, 012009 (2018).
[33] L. P. Chimento and A. S. Jakubi, Classical Quantum Gravity **14**, 1811 (1997).

[34] A. Di Prisco, L. Herrera, and J. Ibáñez, Phys. Rev. D **63**, 023501 (2000).

[35] N. Cruz, A. Hernández-Almada, and O. Cornejo-Pérez, Phys. Rev. D **100**, 083524 (2019).

[36] M. Cruz, N. Cruz, and S. Lepe, Phys. Rev. D **96**, 124020 (2017).

[37] L. Perko, *Differential Equations and Dynamical Systems*, Texts in Applied Mathematics, Vol. 7 (Springer, New York, 2001).

[38] A. R. Liddle and D. H. Lyth, *Cosmological Inflation and Large-Scale Structure* (Cambridge University Press, Cambridge, England, 2000).

[39] V. Mukhanov, *Physical Foundations of Cosmology* (Cambridge University Press, Cambridge, England, 2005).

[40] N. Aghanim, Y. Akrami, M. Ashdown, J. Aumont, C. Baccigalupi, M. Ballardini, A. Banday, R. Barreiro, N. Bartolo, S. Basak *et al.*, Astron. Astrophys. **641**, A6 (2020).

[41] R. F. Sawyer, Phys. Rev. D **39**, 3804 (1989).

[42] P. B. Jones, Phys. Rev. D **64**, 084003 (2001).

[43] M. G. Alford, S. Mahmoodifar, and K. Schwenzer, Phys. Rev. D **85**, 044051 (2012).

[44] M. G. Alford and S. P. Harris, Phys. Rev. C **98**, 065806 (2018).

[45] P. Romatschke, Classical Quantum Gravity **27**, 025006 (2009).

[46] L. Gavassino and J. Noronha, Phys. Rev. D **109**, 096040 (2024).